Novel Heteronuclear Methods of Assignment Transfer from a Diamagnetic to a Paramagnetic Protein: Application to Rat Cytochrome b_5†

R. D. Guiles,*,‡,§,∥ Vladimir J. Basus,§ Siddhartha Sarma,∥ Swati Malpure,∥ Kristine M. Fox,∥ Irwin D. Kuntz,§ and Lucy Waskell*,‡

Department of Pharmaceutical Chemistry, University of California, San Francisco, California 94143, Department of Anesthesia and the Liver Center, University of California, San Francisco, California 94143, Anesthesiology Service, Veterans Administration Medical Center, San Francisco, California 94121, and Department of Biomedicinal Chemistry, School of Pharmacy, University of Maryland at Baltimore, 20 North Pine Street, Baltimore, Maryland 21201

Received March 29, 1993; Revised Manuscript Received May 27, 1993

ABSTRACT: ^{15}N and ^{1}H resonance assignments for backbone and side-chain resonances of both equilibrium forms of rat ferricytochrome b_5 have been obtained, using a combination of novel heteronuclear assignment transfer methods from the known assignments of the diamagnetic protein [Guiles, R. D., Basus, V. J., Kuntz, I. D., & Waskell, L. A. (1992) *Biochemistry 31*, 11365–11375] and computational methods which depend on an accurate determination of the orientation of the components of the susceptibility tensor. The transfer of amide proton resonance assignments takes advantage of the apparent insensitivity of amide ^{15}N resonances to pseudocontact effects, evident in overlays of ^{15}N–^{1}H heteronuclear correlation spectra. Amide-proton resonance assignments tentatively transferred from the known diamagnetic assignments to the paramagnetic form of the protein were confirmed using conventional assignment strategies employing 600-MHz COSY, HOHAHA, and NOESY spectra of the oxidized protein. As was observed in rat ferrocytochrome b_5, more than 40% of all residues exhibited NMR detectable heterogeneity due to the two different orientations of the heme. Complete assignment of both forms enabled accurate determination of the orientation of the susceptibility tensor for both conformations of the heme. The orientation of the z-component of the susceptibility tensors for the two forms are indistinguishable, while the in-plane components appear to differ by about 6°. Differences in the orientation of the in-plane susceptibility components are undoubtedly due dominantly to the relative axial rotation of the heme of between 5° and 10° indicated by the NOESY contacts to the protein observed in the spectra of the ferrocytochrome [Guiles, R. D., Basus, V. J., Kuntz, I. D., & Waskell, L. A. (1992) *Biochemistry 31*, 11365–11375; Pochapsky, T. C., Sligar, S. G., McLachlan, S. J., & LaMar, G. N. (1990) *J. Am. Chem. Soc. 112*, 5258–5263].

Proton chemical shifts of relatively few metalloproteins have been extensively assigned in more than one oxidation state. Cytochrome *c* (Wand et al., 1989; Feng et al., 1989; Gao et al., 1991), bovine cytochrome b_5 (Guiles et al., 1990; Veitch et al., 1990), and thioredoxin (Dyson et al., 1988) are a few notable examples of such systems. The relatively small number of such systems has been due to difficulties caused by (1) efficient relaxation in paramagnetic systems which yields broad lines and, as a result, can severely complicate overlap problems and (2) contact or pseudocontact (dipolar) effects that often result in large shifts in resonance positions resulting in a scrambling of typical connectivity patterns which are the basis of conventional two-dimensional assignment strategies (Wüthrich, 1986). This work focuses on nonisotropic paramagnetic systems with relatively short relaxation times such as heme proteins where both difficulties are encountered.

† Supported by National Institutes of Health Grants GM 35533 (L.W.), DK 46510 (R.G.), GM 19267 (I.K.), and RR 1695 (I.K.) and by a Veterans Administration Merit Review (L.W.). The UCSF Magnetic Resonance Laboratory was partially funded by grants from the National Science Foundation (DMB 9406826) and the National Institutes of Health (RR-01668).

* Correspondence should be addressed to Lucy Waskel, M.D., Ph.D., Veterans Administration Medical Center, Dept. of Anesthesia (129), 4150 Clement St., San Francisco, CA 94121, or Ronald D. Guiles, Ph.D., Dept. of Biomedicinal Chemistry, University of Maryland at Baltimore, 20 North Pine St., Baltimore, MD 21201.

‡ Department of Anesthesia and the Liver Center, UCSF, and VA Medical Center.

§ Department of Pharmaceutical Chemistry, UCSF.

∥ University of Maryland at Baltimore.

Typically, the assignment of a paramagnetic form of a protein must proceed as a separate problem from the assignment of a diamagnetic form of the same protein. However, in a number of cases involving heme proteins, transfer from known diamagnetic assignments has been accomplished using some clever experimental or computational schemes. For example, in studies of mixtures of ferro- and ferricytochrome *c*, Redfield and Gupta (1971) and, more recently, Feng et al. (1990a) have transferred assignments of hyperfine-shifted lines using saturation transfer technqiues. In a few cases [e.g., cytochrome *c* (Feng et al., 1990b; Gao et al., 1991), cytochrome b_5 (Veitch et al., 1990), and myoglobin (Emerson & La Mar, 1990)], it has been possible to determine the orientation of the susceptibility tensor and predict the resonance line shifts of many additional nuclei in the proximity of a paramagnetic center, once a significant number of dipolar-shifted resonances had been assigned.

The pseudocontact or dipolar shift is well-understood theoretically (Kurland & McGarvy, 1970). For a rhombic spin system, the shift Δ_{pc} from an isostructural diamagnetic reference state is given by

$$\Delta_{pc} = [N\beta^2 S(S+1)/9kTr^3][g_{ax}(3\cos^2\theta - 1) + 1.5g_{eq}\sin^2\theta\cos 2\phi] \quad (1)$$

where $g_{ax} = g_z^2 - 1/2(g_x^2 + g_y^2)$, $g_{eq} = g_x^2 - g_y^2$, β is the Bohr magneton, S is the electron spin quantum number, T is the absolute temperature and k is the Boltzmann constant. The position of each proton is defined by its polar coordinates

0006-2960/93/0432-8329$04.00/0

(r,θ,ϕ) relative to the principal axes of the g-tensor (g_x,g_y,g_z). It is generally assumed that room temperature susceptibility components can be calculated from components of the g-tensor derived from low temperature frozen solution or single-crystal EPR spectra using the Van Vleck relation which is implicit in eq 1. However, recently it has been suggested that there may be significant differences in the orientation of these components in room temperature and low temperature measurements (Emerson & La Mar, 1990). Also it is known that second-order Zeeman contributions to the anisotropic susceptibilities are significant at ambient temperatures but do not contribute significantly to g anisotropy at low temperature (Horrocks & Greenberg, 1973; Williams et al., 1985). The axial and equatorial components of anisotropy of the paramagnetic spin systems are defined relative to the principal components of the g-tensor. In this calculation, it is assumed that the unpaired spin density is effectively localized at the metal center which then can be treated as a point dipole. Because of the dependence on distance and orientation, accurate determinations of susceptibility tensor from NMR[1] data (e.g., measured dipolar shifts) have only been possible for systems which have been structurally characterized by other means (e.g., X-ray crystallographically).

Here we present complete assignments of ^{15}N and ^{1}H resonances for both equilibrium forms of rat ferricytochrome b_5. A nearly complete set of assignments for the major abundance form of the bovine ferricytochrome b_5 has been previously reported (Veitch et al., 1990). Assignment of the paramagnetic form of the equilibrium mixture of conformations in the rat cytochrome b_5 was facilitated by novel heteronuclear methods described in detail below. The key to this approach lies in the much smaller apparent sensitivity of ^{15}N resonances to pseudocontact effects relative to ^{1}H resonances. This apparent insensitivity provides a link between the heteronuclear correlation spectra of paramagnetic and diamagnetic forms of the protein which can be exploited in overlays of the spectra. Complete assignment of both diamagnetic (Guiles et al., 1992) and paramagnetic forms of the proteins has enabled accurate determination of the paramagnetic susceptibility tensors for both equilibrium forms of the protein. The existence of differences in the orientation of the tensors for the two conformers of the protein is quite clear from differences in the observed chemical shifts. Calculations of the orientation of the components of the anisotropic susceptibility suggest a difference in the in-plane components which appears to track the observed rotation of the heme in the binding pocket (Guiles et al., 1992; Pochapsky et al., 1990). Our results for the orientation and magnitude of the susceptibility tensor are in reasonable agreement with previous studies of other species variants (Keller & Wüthrich, 1972; Veitch et al., 1990).

Our objective in these studies has been to develop a means of rapidly assigning a protein containing a nonisotropic paramagnetic center using heteronuclear methods and known assignments for an isomorphous diamagnetic system. Then, given assignments of diamagnetic and paramagnetic forms, more accurate susceptibility tensor calculations can be performed. Because the susceptibility calculations are surprisingly accurate and because of the range of these effects (e.g., out to 20 Å), we anticipate that these methods will provide additional distance constraints which should significantly improve the quality of NMR solution structures. Studies to date have used such calculations to determine differences between solution and crystal structures (Veitch et al., 1990), to make stereospecific assignments, and to identify conformational changes between different oxidation states of the protein (Feng et al., 1990b; Gao et al., 1990). These structural and dynamic interpretations are possible because of the abundance of shift data and the excellent reliability of dipolar shift calculations.

[1] Abbreviations: NMR, nuclear magnetic resonance; TSP, sodium (trimethylsilyl)propionante; NOE, nuclear Overhauser effect; NOESY, 2D NOE spectroscopy; COSY, 2D correlated spectroscopy; HMQC, 2D heteronuclear multiple-quantum correlation spectroscopy; HOHAHA, 2D homonuclear Hartman–Hahn spectroscopy; DEPT, distortionless enhancement of polarization transfer; double-DEPT, 2D heteronuclear correlation employing DEPT and reverse DEPT sequences; t_1, evolution time; t_2, data acquisition time; ω_1, Fourier transformed t_1 data; ω_2, Fourier transformed t_2 data; ppm, parts per million.

MATERIALS AND METHODS

Rat Cytochrome b_5: Preparation and Labeling. Unlabeled rat cytochrome b_5 holoprotein was isolated from *Escherichia coli* strain TB-1 harboring a pUC13 plasmid containing the synthetic gene coding for the 98 amino acid polypeptide corresponding to the soluble portion of rat cytochrome b_5 (von Bodman et al., 1986). The plasmid was generously provided by Dr. S. G. Sligar. The bacteria were grown at 37 °C in rich culture media (yeast extract, 10 g/L; bacto-tryptone, 10 g/L; NaCl, 10 g/L). Cytochrome b_5 was isolated using a minor modification of the published procedure (von Bodman et al., 1986). Uniformly ^{15}N-enriched (>99%) protein was obtained by growth of *E. coli* on M9 minimal media (Niedhardt et al., 1974; McIntosh et al., 1987) containing glycerol as a carbon source and $^{15}NH_4Cl$ as the sole source of nitrogen. Expression of the protein in minimal media was found to vary significantly as a function of the host strain of *E. coli*. We found a 20-fold increase in expression on changing host strain from the *E. coli* K-12 host TB-1 to NCM 533, a strain obtained from the laboratory of Dr. H. Boyer at UCSF. Unlike the TB-1 host strain (r^+,m^- derivative of JM83; T. O. Baldwin, Texas A&M; also distributed by Bethesda Research Laboratories) the NCM 533 strain (genotype *lacZ*:TN5, *lacI*^{Q1}, λ^+) is an overproducer of the lac repressor and is not a proline auxotroph (Shand et al., 1991). Expression of the protein was induced by addition of 1 mM IPTG. We obtained 37 mg of purified ^{15}N-labeled cytochrome b_5 from a 12-L culture.

Electrospray mass-spectrometry of both the ^{15}N-enriched and natural abundance proteins indicated that the labeled protein was enriched to greater than 99.7% in ^{15}N. On the basis of the molecular weight determined, we found that the N-terminal methionine coded by the synthetic gene had been posttranscriptionally cleaved. Also, a proteolytic product at about the 10% level was detected. This product corresponded to cleavage between K86 and I87.

NMR Sample Preparation. The purified proteins were desalted over a coarse G-25 column and lyophilized from a 100 mM ammonium bicarbonate solution. The lyophilized cytochrome b_5 samples were dissolved in 100 mM pH 7 phosphate buffers prepared in either 90% H_2O (10% D_2O) or 99.96% D_2O. Cytochrome b_5 samples prepared in 99.96% D_2O buffers were lyophilized twice from 99.96% D_2O prior to dissolution in the final 100 mM phosphate buffer. Small adjustments in the pD to a final value of 7.0 were made by additions of small aliquots of 0.25 M NaOD or DCl. Measurements of pH were not corrected for isotope effects. Trimethylsilyl propionic acid (TSP) was added to a final concentration of 1 mM as an internal chemical shift reference. Cytochrome b_5 concentrations between 5 and 7 mM were used in all NMR experiments. Concentrations of the ferric protein were determined using an absorption coefficient of 117 mM^{-1} at 413 nm (Strittmatter & Velick, 1956).

Two-Dimensional NMR Spectra. NMR spectra were recorded on a 500-MHz General Electric GN-500 NMR spectrometer or at 600 MHz using a General Electric OMEGA PSG600 system. All spectra were recorded in phase-sensitive mode with quadrature detection in both dimensions using a spectral width of 12 500 Hz for protons at 500 MHz and 15 000 Hz at 600 MHz. ^{15}N spectra were recorded with a spectral width of 5000 Hz. All two-dimensional spectra were recorded at 40 °C. Relaxation delay times between 1.2 and 3.5 s were used. NOESY spectra were acquired using the method of States et al. (1982). Mixing times of 100 and 200 ms were used. Double-quantum filtered COSY (Piantini et al., 1982; Shaka & Freeman, 1983) spectra were acquired using time-proportional phase incrementation of the first pulse (Redfield & Kunz, 1975). HOHAHA spectra using the MLEV-17 spin lock sequence (Bax & Davis, 1985) were acquired using high-power proton pulses using a modification developed by Griesinger et al. (1988) which suppresses ROE artifacts. Mixing times of 50, 70, and 100 ms were used. Water suppression in the HOHAHA and NOESY experiments in H_2O was achieved using a DANTE presaturation sequence (Zuiderweg et al., 1986) with a SCUBA modification for recovery of C^α-proton resonances (Brown et al., 1988). Phase-sensitive double-quantum filtered COSY (DQF-COSY) spectra were collected in quadrature using time-proportional phase incrementation (TPPI) (Bodenhausen et al., 1980). DQF-COSY spectra were acquired with 1024 t_1 increments and were zero-filled to 1024 data points with 4096 points in ω_2. All other spectra were acquired with 512 t_1 increments and zero-filled in t_1 to give a real matrix of 1024 points by 2048 points in ω_2.

Double-DEPT sequences (Nirmala & Wagner, 1988) and heteronuclear multiple-quantum coherence (HMQC) sequences (Bax, Griffey & Hawkins, 1983) were used in the acquisition of ^{15}N–proton heteronuclear correlation spectra. In our experience, the double-DEPT experiment has a somewhat lower sensitivity than the HMQC experiment but better resolution than the HMQC, especially for correlation peaks of residues in the β-sheet regions of the protein, because it avoids the secondary amide proton couplings seen in the HMQC experiment. Nitrogen-15 chemical shifts are referenced to an external $^{15}NH_4Cl$ reference standard obtained from Wilmad Corporation (WGN-01) and are reported relative to liquid ammonia. The center of the ^{15}N spectrum was set at the ^{15}N frequency of the D82 amide nitrogen, which is about 128 ppm down field from liquid ammonia. All heteronuclear correlation spectra were recorded with broadband heteronuclear decoupling using the WALTZ-16 sequence (Shaka et al., 1983) during proton detection.

Data Analysis. Two-dimensional NMR spectra were transferred to Sparc workstations (Sun Microsystems, Mountainview, CA) running a UNIX operating system (SunOS 4.1.1). Two-dimensional NMR spectra were processed using software originally developed in the laboratory of Dr. Kaptein at the University of Groningen, Groningen, The Netherlands. Many modifications and improvements have been made by Dr. R. M. Scheek, Dr. S. Manogaran, and Mr. M. Day and Dr. D. Kneller in our laboratory. For all double-quantum filtered COSY experiments, a 70° phase-shifted sine-squared bell was applied. For NOESY and HOHAHA and heteronuclear correlation spectra, Gaussian filters with line-broadening parameters of 6–8 Hz were used. Automatic baseline correction of H_2O spectra were accomplished by an adaptation of an algorithm originally described by Pearson (1977). 600-MHz spectra collected at the University of Maryland, Baltimore County were processed using Felix 2.0 (Hare Research, Woodinville, WA). Spectra were transferred directly from the spectrometer to a Silicon Graphics personal Iris workstation (4D35G) running Irix 3.2.2.

Pseudocontact shift calculations were performed using a set of Fortran programs developed by Dr. S. Donald Emerson and Dr. Gerd LaMar at the University of California, Davis (Emerson & LaMar, 1990). Briefly, the programs SMAX and CALPS calculate dipolar shifts given a set of coordinates for the protein in Brookhaven Protein Databank format, values for the magnitudes of the susceptibility tensor components, and a set of Euler angles defining the orientation of the magnetic axes relative to the molecular axis system of the heme. All angles are defined as described in Emerson and LaMar (1990). A third program, GLOBMIN, performs iterative searches for the orientation of the susceptibility tensor using a least-squares minimization algorithm. As a starting point, susceptibilities were calculated using g values determined from low temperature EPR measurements of the porcine protein [i.e., $g_x = 1.43$, $g_y = 2.23$, and $g_z = 3.30$ (Bois-Poltoratsky & Ehrenberg, 1967)]. However, it should be noted that the susceptibilities calculated in this manner ignore field-dependent second-order Zeeman contributions which are known to be significant at room temperature (Horrocks & Greenberg, 1973). Rather than attempting more exact calculations of anisotropic susceptibility magnitudes from the low temperature g values based on higher order perturbation methods, we simply treated the components of anisotropic susceptibility as adjustable parameters in the minimization of observed-versus-calculated shifts.

RESULTS

The assignment of rat ferricytochrome b_5 involved essentially three steps. First, efficient transfer of many amide proton resonances from the known ferrocytochrome b_5 assignments (Guiles et al., 1992) was accomplished using a comparison of ^{15}N–proton heteronuclear correlation spectra of diamagnetic (ferrocytochrome b_5) forms of the protein. We then confirmed these tentative assignments using conventional sequential assignment procedures employing 600-MHz HOHAHA spectra for confirmation of spin systems and 600-MHz NOESY spectra of the paramagnetic protein for confirmation of connectivities between these spin systems. The third step involved the use of iterative calculations of pseudocontact shifts, which could be used to predict additional resonances once a sufficient number of resonances had been assigned in both diamagnetic and paramagnetic states of the system to enable accurate calculation of the orientation of the susceptibility tensor. Aided by the pseudocontact predictions, assignments of side chain resonances were made on the basis of interpretation of cross-peak patterns in 600-MHz NOESY and HOHAHA spectra. Each of these steps is described in greater detail below.

Transfer of Amide Proton Resonance Assignments Using Overlays of Heteronuclear Correlation Spectra. Although the magnitude of dipolar fields (pseudocontact shifts) is the same for protons and ^{15}N nuclei, the chemical shift dispersion of ^{15}N nuclei is nearly 6 times that of the proton chemical shift range, and thus the pseudocontact shifts for ^{15}N nuclei appear much smaller. Thus, the apparent insensitivity of ^{15}N chemical shifts to pseudocontact effects provides an important link between paramagnetic and diamagnetic forms of the protein which facilitates transfer of amide proton and ^{15}N resonance assignments. It is also important to note that, for many amide proton resonances of residues remote from the

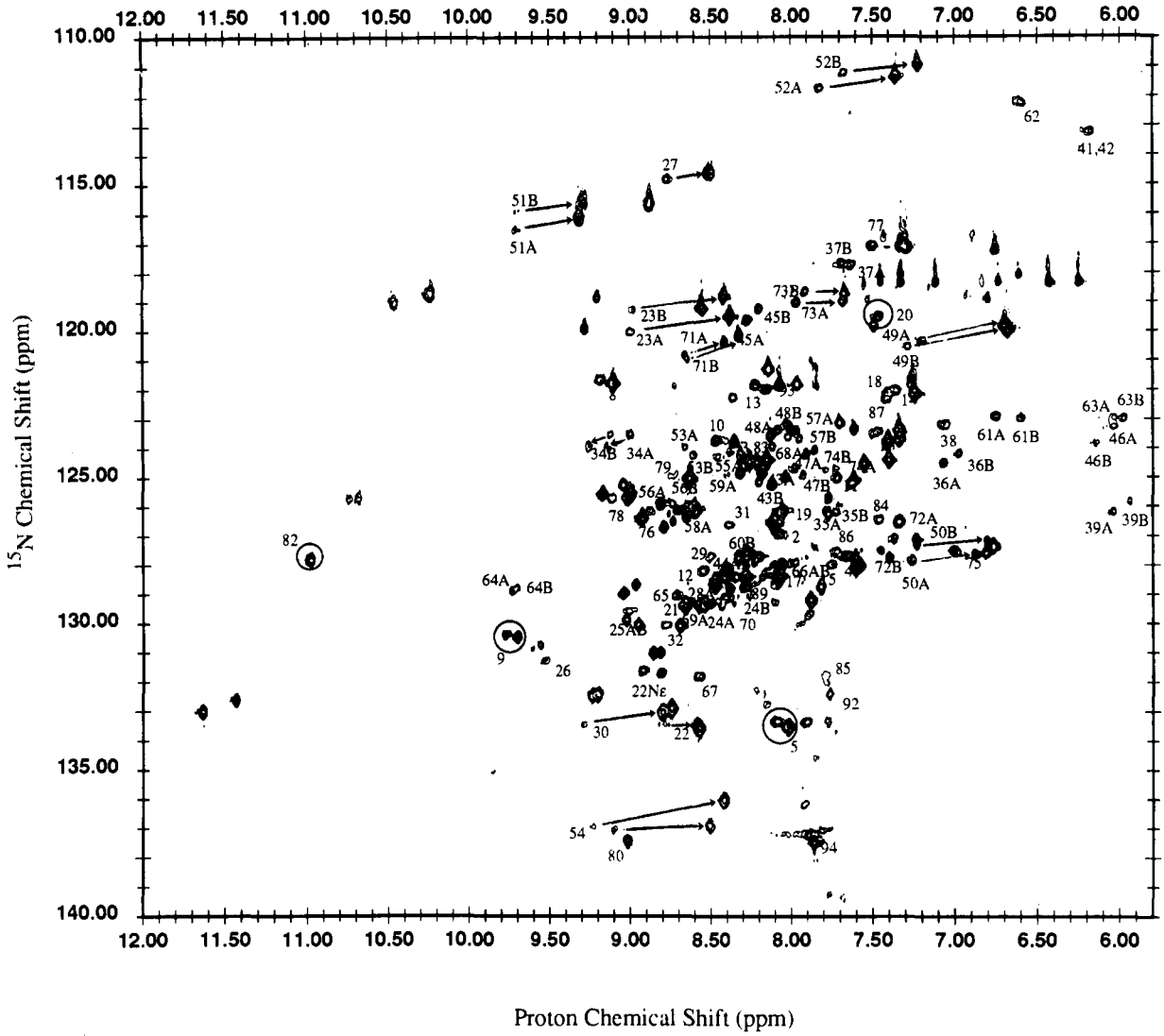

FIGURE 1: Overlay of a contour plot of a ^{1}H–^{15}N heteronuclear correlation spectrum of ferricytochrome b_5 on that of ferrocytochrome b_5. Correlation peaks for ferrocytochrome b_5 are labeled with sequence-specific and conformation-specific resonance assignments. Arrows connecting the known assignments of the reduced protein to the corresponding heteronuclear correlation peaks in the paramagnetic protein are shown for a few peaks which are well resolved in either the ^{15}N dimension or the proton dimension. In many cases, correlation peaks for ferricytochrome b_5 are nearly superimposed on those of ferrocytochrome b_5. Circles have been drawn around a few well-resolved correlation peaks which show small shifts.

paramagnetic center, differences in chemical shift between the ferrocytochrome and the ferricytochrome resonances are small (e.g., D82, K5). Figure 1 contains an overlay of heteronuclear correlation spectra of rat ferricytochrome b_5 and rat ferrocytochrome b_5. Note that the chemical shift range of ^{15}N resonances spans nearly 40 ppm while that of protons is only about 6 ppm. Arrows are drawn from the correlation peak in the diamagnetic protein to the corresponding peak in the paramagnetic protein. For peaks which are well resolved in the ^{15}N dimension (see, for example, G51, G52, T73, S20, and A50 among others), the method is unambiguous. Basically, the comparison of heteronuclear correlation spectra yields a plausible set of amide proton resonance assignments for the oxidized protein, which we subsequently have found to be quite reliable. Note that the slopes of the assignment transfer lines drawn in Figure 1 are all similar, which is not surprising given the difference in the chemical shift ranges plotted and the relative proximity of the proton to its attached ^{15}N. Although virtually every nucleus in the structure is affected to some degree, for many nuclei remote from the heme or at zero crossing points for the dipolar fields the magnitude of the shifts is quite small. For a number of residues, the ^{15}N–^{1}H correlation peaks are nearly superimposed on the overlay. For the sake of illustration, a few well-resolved correlation peaks (e.g., corresponding to K5, L9, S20, D82) with small shifts between diamagnetic and paramagnetic states of the protein have been circled in Figure 1.

Confirmation of Amide Assignment Transfer Using Sequential Connectivity Patterns. Using the amide proton resonances obtained in the previous step as a starting point, sequential connectivities were established through examination of 600-MHz NOESY and COSY and HOHAHA spectra of the paramagnetic protein. The difficulty in assigning severely pseudocontact shifted lines lies in a scrambling of expected orderings of resonances within a given spin system, which confounds conventional spin system assignments using pattern recognition schemes. However, in general, amide, $C^{\alpha}H$, and $C^{\beta}H$ proton resonances can be assigned given the amide ladder in the HOHAHA when used in conjunction with the COSY. Side chains, especially of residues in the heme binding pocket, become more problematic. Once amide $C^{\alpha}H$ and $C^{\beta}H$ protons of a set of spin systems have been assigned, the NOESY connectivities confirm sequential assignments. In this matter,

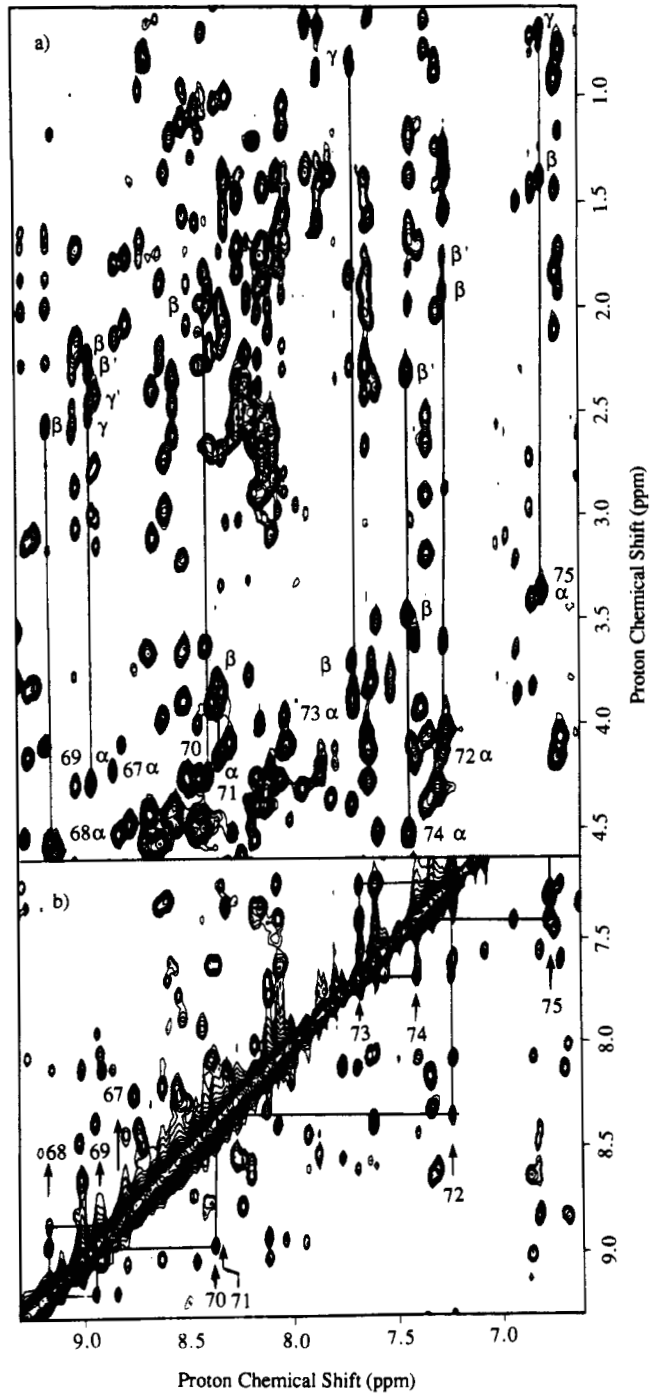

FIGURE 2: (a) Contour plot of the amide region of a 70-ms HOHAHA of a 7 mM solution of rat ferricytochrome b_5 in 90% H_2O/10% D_2O/pH 7.0 phosphate buffer recorded at 600 MHz and 40 °C. (b) Amide–amide region of a 100-ms NOESY spectrum of the same sample recorded at 600 MHz and 40 °C. Vertical lines drawn in panel a define the spin systems, while horizontal amide–amide connectivity line drawn in panel b confirm connectivities predicted by assignment transfer lines shown in Figure 1.

many of the main-chain connectivities of the oxidized (paramagnetic) protein could be transferred.

Despite the size of the protein and the enhanced rate of proton relaxation due to the presence of the paramagnetic center, excellent HOHAHA spectra at 600 MHz were obtained (see Figure 2). In many cases, for example, the majority of the lysines (e.g., K2, K5, K14, K16, K28A,B, K34A,B), complete spin systems were observed. Figure 2 illustrates the confirmation of assignments in displaying the juxtaposition of a 600-MHz NOESY spectrum in the amide–amide region and 600-MHz HOHAHA spectrum in the amide region. Sequential connectivities seen in the NOESY between clearly defined spin systems defined in the HOHAHA confirm the amide assignments transferred using the overlay of heteronuclear correlation spectra shown in Figure 1.

Calculation of the Susceptibility Tensor and Prediction of Side Chain Assignments Using Dipolar Shift Calculations. We used an iterative process to complete the assignments. Once a sufficient number of assignments have been made in both ferrocytochrome b_5 and ferricytochrome b_5, it is possible to calculate the orientation of the susceptibility tensor for the nonisotropic paramagnetic center if the structure is known. In this study we have used the bovine X-ray crystal structure as a model for the rat structures. Magnitudes of the susceptibility components were calculated from components of the g-tensor obtained from low-temperature EPR spectra, using Curie's law (Weissbluth, 1967). Relatively few accurate susceptibility tensor calculations have been performed to date due to a lack of extensive assignments in paramagnetic and diamagnetic reference states. As a starting point, tensor calculations were performed on the basis of amide assignments in both states. It is also implicitly assumed that the structures in oxidized (paramagnetic) and reduced (diamagnetic) states are nearly identical. This is a reasonable assumption for cytochrome b_5 (Argos & Mathews, 1975), although there have been some indications of differences between the solution and crystal structures reported for the bovine protein (Veitch et al., 1990).

Once the orientation of the susceptibility tensor has been obtained, predictions of all other resonances of the paramagnetic protein are possible, if the assignments are known for the ferrocytochrome. These predictions were used to guide assignments based on COSY and HOHAHA spectra of the oxidized protein. Once assignments had been unambiguously established with this larger set of known assignments, more accurate susceptibility tensors could be calculated and used to more accurately predict side chain or severely shifted amide resonance assignments. Figure 3 contains the same overlay shown in Figure 1 but now illustrates transfer of some severely shifted amide resonances based on pseudocontact shift calculations. This process was repeated until a full set of assignments was obtained.

Assignments of Both Equilibrium Forms of Rat Ferricytochrome b_5. As was the case for ferrocytochrome b_5, two nearly equally abundant equilibrium conformations of the cytochrome exist which differ by a 180° rotation of the heme about the α,γ-meso axis. Assignment of each equilibrium form proceeded essentially independently, although differences in overlap patterns of the parallel NOESY connectivities or amide HOHAHA ladders were often invaluable aides in assignment. As with the ferrocytochrome, more than 40% of the protein displays distinguishable resonances due to each conformation. Figure 4 is the fingerprint region of a ^{15}N–proton heteronuclear correlation spectrum with a full set of sequence and conformation specific assignments. Doubling of many of the correlation peaks for residues in the vicinity of the heme is evident in this spectrum.

Ultimately, as was the case with ferrocytochrome b_5, conformation-specific assignments were established using unique heme–proton to protein–proton NOESY connectivities. Once established for a number of residues, continuous unambiguous sequential connectivities propagated conformation-specific assignments. Heteronuclear correlation spectra played a key role in assignment for two reasons: (1) The superior sensitivity of heteronuclear correlation spectra reliably

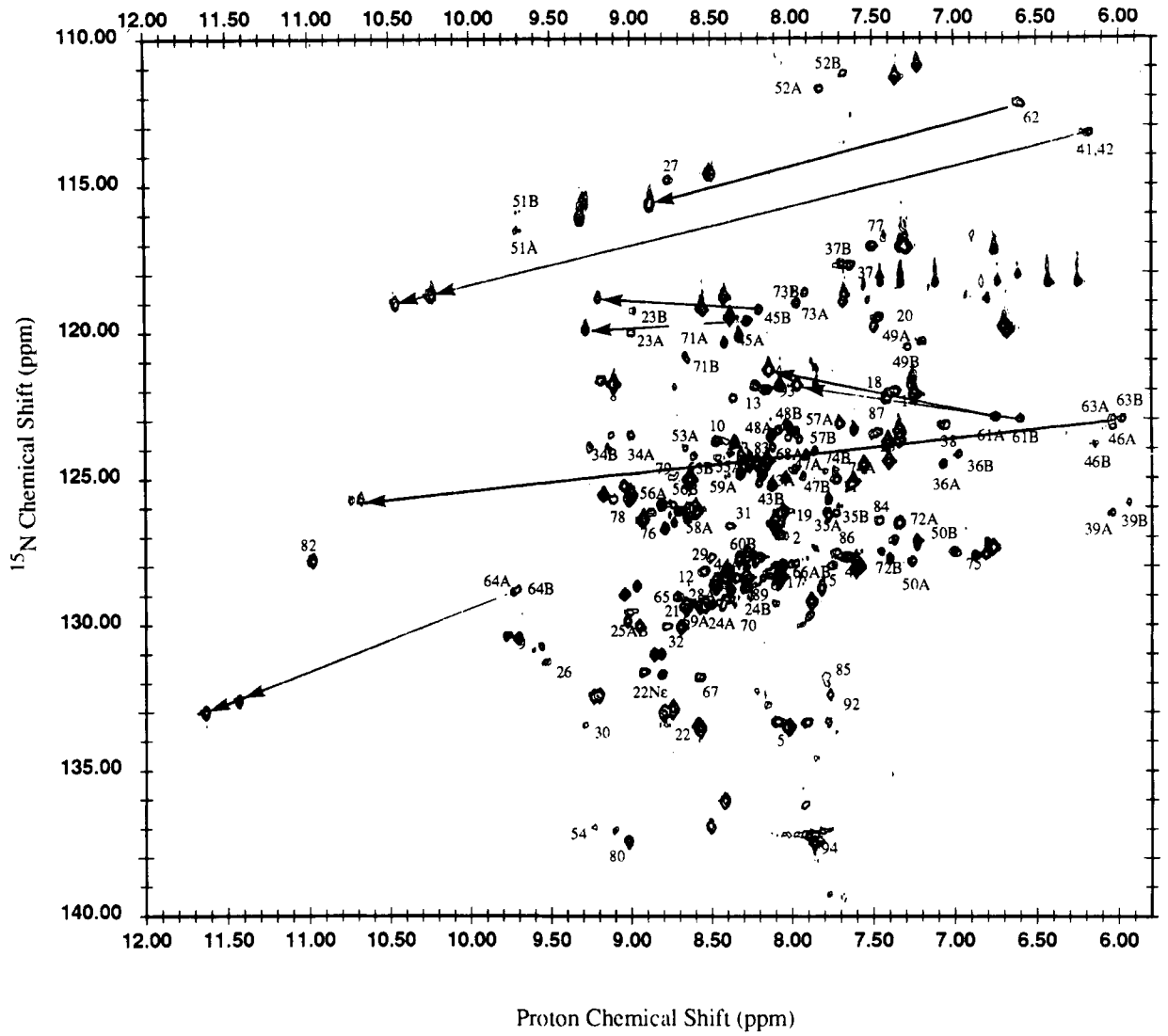

FIGURE 3: Relationship between assigned correlation peaks in paramagnetic and diamagnetic forms of cytochrome b_5 are indicated by arrows connecting the reduced to the oxidized form. The assignments for the oxidized protein were predicted on the basis of pseudocontact shift calculations and later confirmed by conventional assignment strategies such as those indicated in Figure 2.

yielded cross-peaks for virtually all residues in the protein. This of course enabled the transfer of assignments from the diamagnetic state of the protein using the methods described above. Considering the variation in peak width as a result of variable paramagnetic relaxation, sensitivity is an important property of heteronuclear correlation spectra. (2) The large ^{15}N dispersion is also a significant factor in obtaining unique assignments of nonoverlapping correlation peaks. In many cases, the increased dispersion of proton resonances of the paramagnetic protein due to pseudocontact effects also assisted in resolving overlap problems. A complete set of ^{15}N and proton resonance assignments for both equilibrium forms of rat ferricytochrome b_5 is contained in Table I.

It was clear at an early stage in the analysis that the two conformers had significantly different tensor orientations from differences in the magnitude of dipolar shifts in resonances of certain residues. For example, some residues which exhibited a single correlation peak in the reduced form split significantly in the oxidized form (see, for example, H26, Y30, G42, I75). Also, some residues exhibited heteronuclear correlation peaks which showed clear conformational differences in the reduced form, collapse to a single correlation peak in the oxidized form (see, for example, E37 and Q49).

Progressive refinement of susceptibility tensor orientations for both equilibrium forms of the protein revealed apparent differences between the two conformations. Once complete assignments for both equilibrium forms had been obtained, final optimized tensor orientations for each equilibrium conformer were obtained using a set of 45 amide reference protons. Reference protons were selected using the following criteria. In order to minimize uncertainty due to redox-dependent structure changes or violations of the dipole approximation, only protons more than 7 Å from the heme iron were utilized. The largest possible shifts were used. In order to obtain the best possible discrimination of differences between tensor orientations, residues were selected which displayed the largest differences in dipolar shifts between the two conformations. Table II contains susceptibility tensor parameters for the two different conformations of the heme obtained using this set of data.

Clearly the differences between the orientation of the z-components of the anisotropic susceptibility tensor are insignificant. Well-defined minima for the two different tensors are suggestive of a difference in the in-plane components of approximately 6°. It is interesting to note that both the direction and magnitude of this in-plane shift are consistent with the rotation of the heme that Guiles et al. (1992) and Pochapsky et al. (1990) have previously suggested on the basis of the interpretation of protein-to-heme NOE contacts observed in the ferrocytochrome b_5. However, based

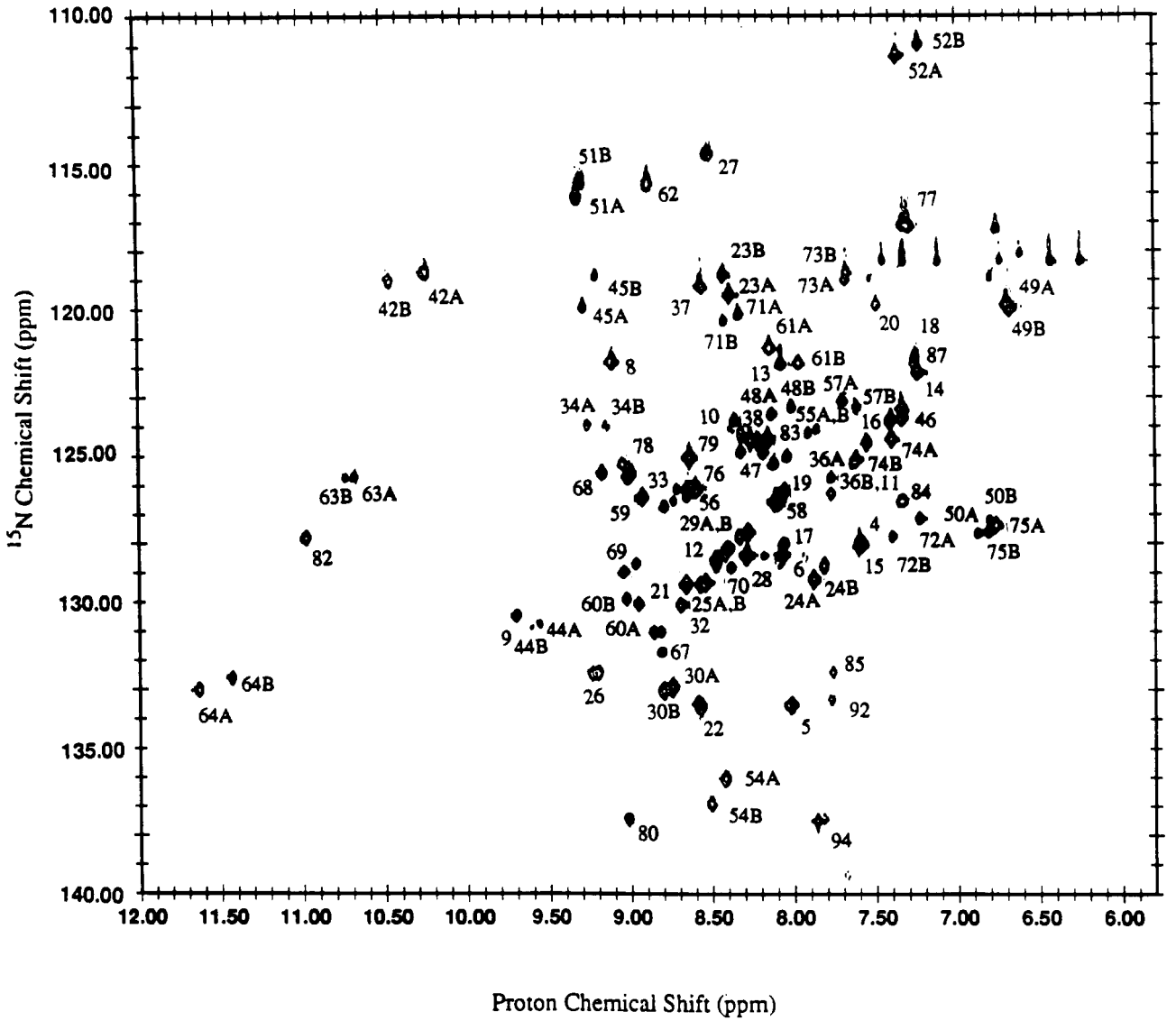

FIGURE 4: Contour plot of an ^{15}N–^{1}H heteronuclear correlation spectrum of ferricytochrome b_5. Complete sequence-specific and conformation-specific assignments are indicated in the figure. The spectrum is a 500-MHz HMQC spectrum of a 7 mM solution of ferricytochrome b_5 in 90% H_2O/10% D_2O/pH 7.0 phosphate buffer recorded at 40 °C.

on a detailed analysis of the variation of the least-square residual as a function of the difference in in-plane angular orientation (shown in Figure 5), the statistical significance of this difference is weak. This suggests that other redox-linked shift variation may limit our ability to determine the orientation of two different susceptibility tensors accurately enough to discriminate angular differences of this magnitude.

Linear regression plots of calculated versus observed shifts for both final optimized tensor orientations are shown in Figure 6. Regression parameters are shown for the complete set of data displayed, although it should be noted that many of the significant deviations from the linear relationship occur systematically for the same residues in both conformations, indicating that the observed deviations are not statistical in nature but are due to a breakdown in one of the assumptions implicit in eq 1. In previous studies, such differences have been attributed to differences between the structures of oxidized and reduced proteins (Feng et al., 1990b) or differences in dynamics of residues in the solid state (e.g., the crystallographic coordinates were used in the calculation) and in solution. For protons which show large pseudocontact shifts, the deviations are often the largest. However, because these nuclei are closer to the paramagnetic center, the point dipole approximation begins to break down, and multipole effects or the effects of delocalization of the unpaired electron spin become significant. It has previously been estimated that the lower bound for the validity of treating the unpaired spin system as a point dipole is approximately 7 Å (Golding & Stubbs, 1979). Thus, a more accurate determination of the orientation of the components of the susceptibility tensor is obtained by using shifts for nuclei at distances greater that 7 Å from the heme iron.

In the calculation of the orientation of the susceptibility components of both conformations of the heme, the reference molecular axis system used was the major abundance conformation or A-form determined in the bovine crystal structure (Mathews et al., 1972). Differences in the angular orientation of the in-plane components (6°) appear to confirm earlier predictions of an additional axial rotation of the heme in the binding pocket of between 5° and 10° (Guiles et al., 1992; Pochapsky et al., 1990). Figure 7 depicts the orientation of the magnetic axes for the in-plane components for both conformations.

Prediction of Redox Shifts in ^{15}N Resonance Frequencies Using Dipolar Shift Calculations. In principle, pseudocontact shifts can be calculated as accurately for ^{15}N nuclei as for protons; however, in practice the predictions are less accurate. For example, the redox linked ^{15}N shifts indicated in Figure

Table I: Summary of Sequence-Specific Assignments for Both Equilibrium Conformations of Rat Ferricytochrome b_5

residue[a,b]	^{15}N	NH	$C^{\alpha}H$	$C^{\beta}H$	$C^{\beta'}H$	other assignments
D1	124.4	8.27	4.52	2.64		
K2	126.6	8.09	4.30	2.05		1.43(γ) 1.68(δ) 3.01(ϵ)
D3	124.4	8.16	4.55	2.53		
V4	127.7	7.59	3.78	1.57		0.63(γ) 0.32(γ')
K5	133.5	8.00	4.07	1.58		1.16(γ) 1.03(γ') 1.58(δ) 2.79(ϵ) 2.88 (ϵ')
Y6	128.4	8.06	5.64	2.82	2.59	6.84(δ) 6.62(ϵ)
Y7	125.0	8.62	5.12	3.12	2.42	6.86(δ) 6.56(ϵ)
T8	121.8	9.13	4.60	4.81		1.19(γ)
L9	130.4	9.70	3.96	1.68	1.45	1.64(γ) 0.97(δ) 0.89(δ')
E10	123.8	8.35	3.88	2.20	1.91	2.26(γ) 2.18(γ')
E11	125.2	7.61	4.02	2.42	2.28	2.65(γ)
I12	128.2	8.37	3.60	1.87		2.02(γ) 0.73(γ') 1.01(γCH_3)
Q13	121.9	8.07	4.22	1.98	2.12	2.51(γ)
K14	122.1	7.23	4.04	1.37		1.25(γ) 1.54(δ) 2.87(ϵ)
H15	128.1	7.60	4.13	2.35	1.52	6.72(δ) 7.89(ϵ)
K16	123.8	7.42	4.72	1.38		1.18(γ) 1.70(δ) 3.02(ϵ)
D17	128.0	8.06	4.92	3.10	2.68	
S18	120.2	7.39	4.69	4.09		
K19	126.2	8.04	4.27	1.79		1.39(γ) 1.70(γ) 2.99(ϵ)
S20	119.8	7.48	5.00	3.83	3.78	
T21	129.4	8.66	4.44	3.66		0.82(γ)
W22(A)	133.6	8.58	6.16	2.97	2.73	6.82(δ_1) 6.59(ϵ_3) 6.67(ζ_2) 5.82(ζ_3) 6.39(η_2) 8.81(ϵ_1) 131.7($^{15}N\epsilon_1$)
W22(B)	133.6	8.59	6.18	2.99	2.72	6.81(δ_1) 6.59(ϵ_3) 6.69(ζ_2) 5.83(ζ_3) 6.43(η_2) 8.81 (ϵ_1) 131.7($^{15}N\epsilon_1$)
V23(A)	119.4	8.39	4.47	1.20		–0.13(γ) –0.37(γ')
V23(B)	118.8	8.42	4.48	1.29		–0.04(γ) –0.30(γ')
I24(A)	129.2	7.87	4.97	1.38		0.67(γ) 0.51(γ')
I24(B)	128.7	7.82	5.02	1.46		0.69(γ) 0.55(γ')
L25(A)	129.3	8.55	4.40	1.20	0.21	–0.01(γ) –0.78(δ) –1.96(δ')
L25(B)	129.4	8.58	4.55	1.38	0.25	0.07(γ) –0.58(δ) –1.78(δ')
H26(A)	132.4	9.21	3.81	3.10		6.92(δ) 8.05(ϵ)
H26(B)	132.4	9.23	3.83	3.12		6.99(δ) 8.07(ϵ)
H27	114.5	8.50	3.89	3.63	3.20	6.86(δ) 7.83(ϵ)
K28(A)	128.8	8.26	4.86	1.72		1.51(γ) 1.85(δ) 3.02(ϵ)
K28(B)	129.8	8.28	4.77	1.53		1.36(γ) 1.62(δ) 3.02(ϵ)
V29(A)	127.6	8.27	4.08	1.01		0.53(γ) 0.00(γ')
V29(B)	127.8	8.32	4.17	1.04		0.52(γ) 0.02(γ')
Y30(A)	132.8	8.74	4.47	2.08	1.76	6.52(δ) 7.06(ϵ)
Y30(B)	133.0	8.79	4.52	2.15	1.79	6.57(δ) 6.87(ϵ)
D31(A)	125.2	8.05	4.90	2.86	2.65	
L32	130.1	8.73	4.46	1.39		0.65(γ) –0.18(δ) –0.40(δ')
T33	126.5	8.71	4.33	4.23		1.25(γ)
K34(A)	123.9	9.14	4.58	2.25	2.00	1.70(γ) 1.62(γ') 1.88(δ) 3.18(ϵ)
K34(B)	123.9	9.25	4.54	2.27	2.01	1.70(γ) 1.62(γ') 1.88(δ) 3.18(ϵ)
F35(A)	126.5	8.11	5.14	2.75	2.62	7.42(δ) 8.21(ϵ) 7.67(ζ)
F35(B)	126.2	8.04	5.01	2.71	2.63	7.38(δ) 8.23(ϵ) 7.67(ζ)
L36(A)	125.7	7.77	4.71	2.34		2.04(γ) 1.79(δ) 1.69(δ')
L36(B)	125.4	7.62	4.65	2.33		2.04(γ) 1.79(δ) 1.69(δ')
E37	119.2	8.53	4.83	2.47	2.35	2.61(γ)
E38(A)	124.4	8.27	4.86	2.45	2.37	2.61(γ)
E38(A)	124.4	8.23	4.83	2.43	2.35	2.61(γ)
H39(A)	131.00	8.77	4.69			
P40						
G41						
G42(A)	118.7	10.23	5.95			5.63(α')
G42(B)	119.0	10.48	6.09			5.75(α')
E43(A)	127.6	9.92	5.77	2.83	2.75	
E43(B)		9.97	45.73	2.81	2.76	
E44(A)	128.8	9.57	4.25	2.48	2.35	2.63(γ)
E44(B)	128.9	9.61	4.23	2.48	2.35	2.61(γ)
V45(A)	119.9	9.27	4.15	2.49		1.29(γ) 1.21(γ')
V45(B)	118.8	9.18	4.08	2.46		1.26(γ) 1.16(γ')
L46	123.3	7.32	3.18	2.66	2.52	0.78(δ) 0.64(δ')
R47(A)	124.8	8.32	3.86	1.99		1.76(γ) 3.34(δ)
R47(B)	124.8	8.18	3.77	1.98		1.72(γ) 3.32(δ)
E48(A)	123.6	8.13	3.99	2.02		2.36(γ)
E48(B)	123.4	8.01	3.95	1.95	1.80	2.29(γ)
Q49(A)	119.8	6.69	4.12	1.43	0.91	2.11(γ) 1.93(γ')
Q49(B)	120.0	6.67	4.06	1.18	0.73	1.93(γ) 1.72(γ')
A50(A)	127.6	6.87	3.84	1.50		
A50(B)	127.2	6.80	3.79	1.45		
G51(A)	116.1	9.32	3.82			3.53(α')
G51(B)	115.5	9.28	3.78			3.55(α')
G52(A)	111.4	7.36	4.16			3.58(α')
G52(B)	110.8	7.22	4.12			3.59(α')
D53(A)	124.4	8.30	4.52	2.65		
D53(B)	124.3	8.35	4.45	2.70		
A54(A)	136.0	8.42	4.48	0.16		

Table I (Continued)

residue[a,b]	^{15}N	NH	$C^{\alpha}H$	$C^{\beta}H$	$C^{\beta'}H$	other assignments
A54(B)	136.9	8.53	4.48	0.28		
T55(A)	124.2	7.92	2.93	3.85		0.49(γ)
T55(B)	124.0	7.84	2.94	3.88		0.46(γ)
E56	124.3	8.58	4.45	2.56	1.87	
N57(A)	121.2	7.66	4.35	2.26	1.84	
N57(B)	121.4	7.59	4.26	2.26	1.82	
F58(A)	123.3	8.13	3.98	2.97	2.01	
F58(B)	123.1	8.00	3.94		1.92	
E59	126.4	8.89	5.43	2.77	2.41	3.16(γ) 3.02(γ′)
D60(A)	129.8	9.01	4.84	3.06	2.86	
D60(B)	130.0	8.93	4.81	2.98	2.76	
V61(A)	121.3	8.10	4.38	2.75		1.85(γ)
V61(B)	121.8	7.93	4.37	2.78		1.88(γ)
G62(A)	115.6	8.85	5.00			
H63(A)	125.6	10.69				
H63(B)	125.7	10.74				
S64(A)	133.0	11.63	4.95	4.57	4.25	
S64(B)	132.6	11.43	4.91	4.45	4.16	
T65	126.7	8.81	4.92	2.88		0.64(γ)
D66	122.5	8.27	4.48	2.64	2.54	
A67(A)	131.0	8.83	4.22	1.64		
A67(B)	131.0	8.79	4.09	1.54		
R68(A)	127.6	9.16	4.46	2.74	2.56	3.00(δ)
R68(B)	125.2	9.00	4.54	3.05	2.85	2.55(γ)
E69(A)	128.2	8.93	4.26	2.28		2.53(γ) 2.46(γ′)
E69(B)	127.9	9.01	4.27	2.31		2.54(γ)
L70(A)	128.8	8.36	4.23	2.00		1.81(γ) 1.00(γ′) 0.69(δ)
L70(B)	128.8	8.47	4.27	2.06	1.87	1.58(γ) 1.11(γ′) 0.96(δ)
S71(A)	120.2	8.31	3.92	3.80		
S71(B)	120.4	8.41	4.01	3.90		
K72(A)	127.1	7.23	4.01	1.91	1.75	
K72(B)	127.7	7.39	4.12	1.98	1.79	
T73(A)	119.0	7.67	3.85	3.69		0.84(γ)
T73(B)	118.7	7.67	3.92	3.85		0.88(γ)
Y74(A)	124.5	7.39	4.52	3.47	2.32	6.93(δ) 6.37(ε)
Y74(B)	124.5	7.55	4.51	3.49	2.38	7.09(δ) 6.52(ε)
I75(A)	127.4	6.76	3.35	1.35		1.21(γ) 0.76(γ′) 0.68(δ) −0.22 (γCH_3)
I75(B)	127.6	6.80	3.39	1.41		1.25(γ) 0.78(γ′) 0.64(δ)
I76(A)	126.0	8.59	4.56	1.73		0.63(γ) 0.08(γ′) −0.13(γCH_3) −1.12(δ)
I76(B)	126.1	8.64	4.58	1.73		0.65(γ) 0.09(γ′) −0.12(γCH_3) −1.12(δ)
G77	117.1	7.28	4.36			4.04(α′)
E78	125.6	8.89	5.01	1.70		
L79	125.0	8.62	4.56		0.64	
H80	137.4	9.01	3.74	2.84	2.53	6.98(δ) 7.63(ε)
P81						
D82	127.8	10.98	4.47	2.63		
D83	122.3	8.16	4.90	2.91	2.61	
R84	126.5	7.34	3.92	2.64	1.70	
S85	132.4	7.78	4.27			
K86	127.8	7.60	4.26	2.25	1.90	1.36(γ)
I87	121.6	7.26	4.27	2.00	1.40	1.21(γ) 0.88(γ′)
A88	126.2	7.78	4.29	1.37		
K89	128.6	8.47				
P90						
S91						
E92	133.4	7.78	4.19	1.68		2.45(γ)
T93	121.3	8.11	4.38	3.99		1.21(γ)
L94	137.4	7.84	4.22	1.61		0.90(δ)

[a] Amino acid sequence taken from von Bodman et al. (1986). When separate conformation specific resonances could be umabiguously assigned, the letters A and B are used to specify the particular conformation. The amino acids are referred to by their single-letter symbols. [b] Proton chemical shifts are referenced to TSP, and ^{15}N chemical shifts are reported relative to ammonia.

1 are predicted much less accurately than the corresponding proton shifts. The correlation coefficient for the predicted versus measured ^{15}N dipolar shifts is 0.822. The larger shifts show much lower correlations. This simply indicates that there are other factors which effect ^{15}N chemical shifts which are dependent on the oxidation state of the protein. This is not surprising given the enormous sensitivity of ^{15}N chemical shifts to subtle changes in chemical structure. Nitrogen-15 chemical shifts span a range of 1000 ppm, which is five times the range observed for carbon-13 shieldings (Bovey, 1988). The amide ^{15}N chemical shift range alone spans nearly 40 ppm. There have been several attempts to obtain information from the variation in ^{15}N chemical shifts (Llinás et al., 1976; Kricheldorf, 1981; Glushka et al., 1989). While it is clear that solvation, hydrogen bonding, and the planarity of the peptide bond must play key roles in determining the chemical shifts, as yet only weak correlations have been observed with any given parameter. In the context of this work, these other sources of redox dependent shift variation just serve to reduce the reliability of dipolar shift predictions for ^{15}N resonances, and perhaps to some degree may be useful in suggesting regions were subtle changes in structure may be occurring. For example, in Figure 3 the anomalous slopes of the assignment transfer lines for residues 23, 61, and 64 suggest that redox-

Table II: Components of the Susceptibility Tensor for Both Equilibrium Conformations[a]

	conformations	
	A	B
$\Delta\chi_{ax}$	1643×10^{-12}	1643×10^{-12}
$\Delta\chi_{rh}$	-847×10^{-12}	-847×10^{-12}
α	23.0	25.0
β	8.0	9.0
γ	0.0	4.0

[a] Axial and rhombic components of the anisotropic susceptibility and Euler angles are defined as described by Emerson and LaMar (1990). Susceptibilities are expressed in Van Vleck units (m^3/mol) Horrocks and Hall (1971). Euler angles are in degrees.

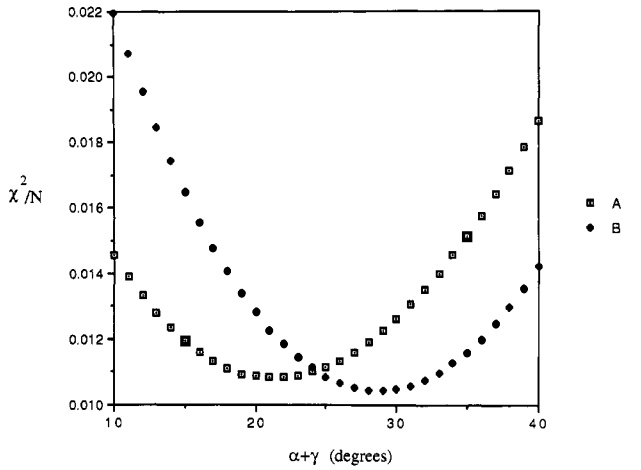

FIGURE 5: Variation in the least-square residual for calculated versus observed shifts as a function of the in-plane angular difference between the molecular and magnetic axes ($\alpha+\gamma$). The heme molecular axis system is defined as described by Emerson and La Mar (1990). The plot shown is a least-square residual of differences between observed and calculated dipolar shifts; $\chi^2/N = \sum(\Delta_{obs} - \Delta_{calc})^2/N$. For the A form of the protein, α and β were held constant at the best fit values of 23.0° and 8.0°, respectively, while γ was systematically varied from −13.0° to +17.0°. For the B form, α and β were fixed at the best fit values of 25° and 9°, respectively, and γ was varied systematically in 1° increments from −15° to +15°.

linked structural changes may be occurring at these sites. This is perhaps not surprising given the proximity of these residues to the heme.

DISCUSSION

We have explored the use of heteronuclear two-dimensional methods in the application to a metalloenzyme system which exhibits dipolar shift effects. The relative insensitivity of ^{15}N resonances to pseudocontact effects provides a link between assignments for the diamagnetic reference system (ferrocytochrome b_5) and the paramagnetic form of the protein. The utility of these methods in allowing rapid transfer of assignments should as a result enable studies of more complex systems which exhibit dipolar shift effects.

In principle, long-range dipolar shifts can be measured more accurately than other effects which can be used as structural constraints. Because dipolar fields induce shifts in line positions, usually relative to a well-defined reference state (e.g., some diamagnetic reference, in this case ferrocytochrome b_5), they can be measured to a high degree of accuracy. This is in contrast to paramagnetic relaxation effects, which are measured as differential line-broadening effects. On the other hand, other effects which induce line shifts, and thus in principle can be measured with a high degree of accuracy, suffer from difficulties in the definition of the exact resonance

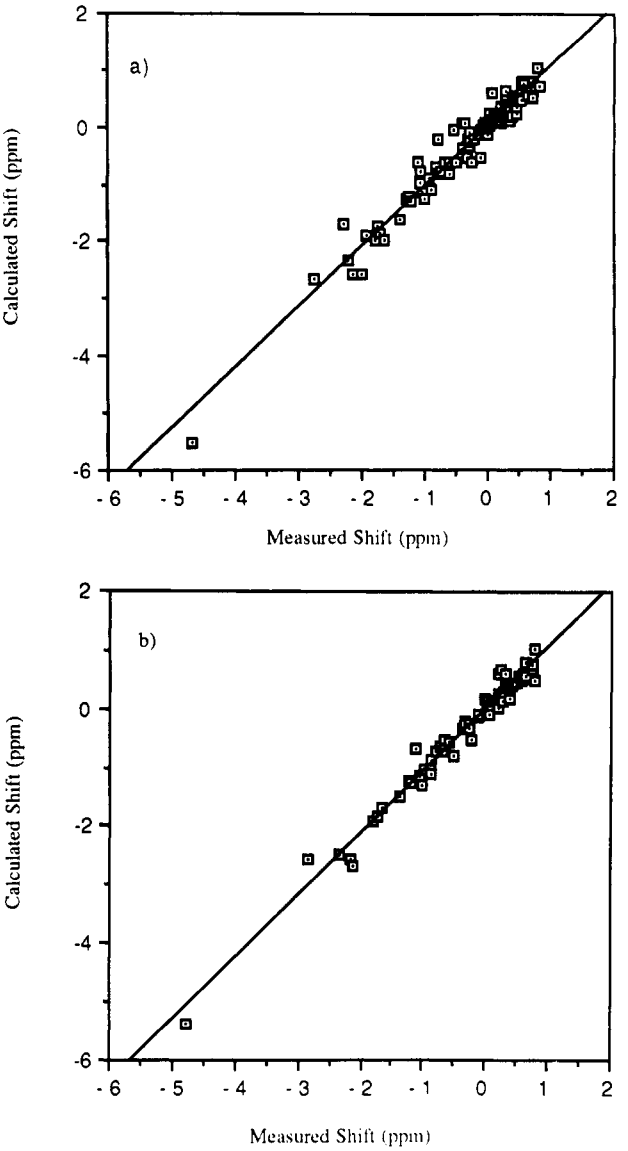

FIGURE 6: (a) Linear regression plot of calculated versus observed dipolar shifts for the amide and C^α protons of the A form of rat cytochrome b_5 and (b) amide and C^α protons of the B form. The regression parameters for the least-squares fit to the 157 points plotted in panel a are as follows: slope = 1.055, intercept = 0.01, and R^2 = 0.955. The regression parameters for the least squares fit to the 83 points plotted in panel b are as follows: slope = 1.062, intercept = 0.0004, and R^2 = 0.997. Only amide and C^α protons which differed by more than 0.02 ppm between the two different conformations are plotted in panel b. Calculated values in each case are based on the susceptibility parameters contained in Table II.

position of the reference state. For example, the reference state usually used in ring-current calculations is the free chain [tabulations commonly used are actually in the form of specific positions in tetrapeptides, e.g., Bundi and Wüthrich (1979)]. Note that use of distance constraints obtained from paramagnetic relaxation have a long history and continue to be used (Villafranca, 1989). Recent improvements in the calculation of ring-current effects suggest that they may also be of use as constraints in the calculation of solution structures (Gippert et al., 1990; Ösapay & Case, 1991) especially for systems which exhibit large ring-current effects (e.g., heme proteins and proteins containing a significant number of tryptophans).

Dipolar shifts have a number of unique properties which can potentially be exploited effectively as constraints in the refinement of NMR solution structures. First, the dipolar

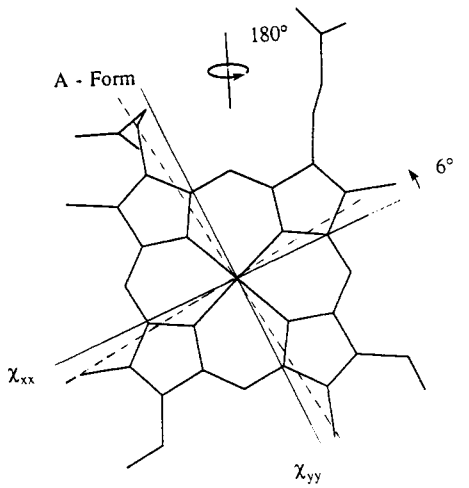

FIGURE 7: Orientation of the in-plane components of magnetic susceptibility (χ_{xx} and χ_{yy}). The solid axes represent the principle components of the A form. The dashed lines represent the orientation of the χ_{xx} and χ_{yy} in the B form overlayed on the the orientation of the heme in the A configuration. In the view of the heme shown, H63 would be coming out of the plane of the page. As described previously (Guiles et al., 1992; Pochapsky et al., 1990) the heme in the B configuration relative to the A form is flipped about the α,γ-meso axis (as shown) and also rotated 5–10° about the heme-plane normal. The axial rotation of the heme about its normal is consistent with the rotation of the axes shown.

shift depends solely on the distance of a given nucleus from the paramagnetic center and the orientation of that nonisotropic paramagnetic center relative to the nucleus of interest (Bertini & Luchinat, 1986). The dipolar shift does not directly depend on the relaxation rate of the paramagnetic center, a parameter which is difficult to directly determine at ambient temperatures. The range of the effect is enormous compared to other physical effects commonly used as constraints in NMR (e.g., NOE and coupling constant constraints). Significant dipolar shifts can be observed out to 20 Å from the paramagnetic center.

Unfortunately, large dipolar shifts are only observed for a limited number of metal-based paramagnetic systems. This is due to two physical requirements which must be properties of the paramagnetic system under investigation: (1) the paramagnetic center must exhibit a high degree of magnetic anisotropy, and (2) the relaxation rate of the paramagnetic center must be fast. These requirements are met in low-spin ferric heme systems, in cobalt(II) systems, and in systems containing certain lanthanide ions (e.g., Yb^{3+}, Dy^{3+}). In the case of the latter two metal systems, these ions have been used as isomorphous paramagnetic replacements for endogenous diamagnetic metal centers. For example, Co^{2+} is often used as a paramagnetic replacement for Zn^{2+} in Zn proteins (Bertini & Luchinat, 1986). Similarly, because the trivalent lanthanides have an ionic radius similar to that of calcium(II), they have been used extensively as isomorphous replacements in calcium-binding proteins (Lenkinski, 1984).

In this work we have found a unique system in which distinguishable susceptibility tensors exist in a system of two slowly exchanging equilibrium conformations. It is also known that the two different conformations of the cytochrome have midpoint potentials which differ by nearly 30 mV (Walker et al., 1988). Given this difference, it is probable that NMR solution studies of this system will yield insights into the nature of protein–heme recognition factors which control midpoint potentials in cytochromes.

NMR methods provide two essential components necessary for a complete understanding of protein–heme recognition factors which mediate differences in midpoint potential among cytochromes. First, high-resolution solution methods are uniquely capable of yielding detailed solution structures for both equilibrium conformations. Second, the susceptibility tensor determinations, coupled with calculations of the magnitude of anisotropy and the level of noncoincidence of magnetic and molecular axis systems, should provide important probes into how heme orbital energy levels are being perturbed in the protein environment.

It has been possible to fully assign both equilibrium forms of the protein in both paramagnetic and diamagnetic states of the system because of a powerful range of heteronuclear experiments applied to the isotopically enriched protein. Given this complete set of assignments, a set of independent constraints for each structure should permit structural elucidation of both forms. The high sensitivity and enhanced dispersion of heteronuclear methods not only allowed complete assignment of this extraordinarily heterogeneous system (Guiles et al., 1992) but also permitted novel methods of assignment transfer from the diamagnetic to the paramagnetic form.

The physical origins of magnetic anisotropy are reasonably well understood in terms of spin orbit coupling to exited state electronic configurations (Keijzers & de Boer, 1975a,b; Scullane et al., 1979). Also, ground state orbital mixing of nondegenerate heme oribtals in the cytochrome which are forbidden in the free heme induce the large angles of noncoincidence between magnetic and molecular axis systems. Both of these effects are sensitive functions of separations of heme orbital energy levels (Emerson & LaMar, 1990). Hence they are also indicators of heme midpoint potentials in a given environment, in that the heme orbital levels are key determinants of the midpoint potential of the cytochrome. Thus, the combination of detailed structural elucidation using NMR solution methods coupled with detailed orbital calculations of the magnetic properties of the heme should yield insights into the nature of protein regulation of heme midpoint potentials. The studies presented here suggest that the main differences in the orientation of the susceptibility tensors exhibited by the two conformations are due to differences in the orientation of the heme itself in the binding pocket (e.g., the tensor components appear to simply track the orientation of the heme). This is perhaps surprising in that the magnitude of noncoincidence of molecular and magnetic axes is a sensitive function of heme orbital energy levels and in this case appears to be insensitive to the orientation of the axial histidines. This suggests that differences observed in the midpoint potentials are not due to shifts in heme orbital energy levels of the ferricytochrome. However, until we obtain high-resolution solution structures of both equilibrium forms of the rat cytochrome, these observations remain speculative.

ACKNOWLEDGMENT

Solvent electrospray mass spectrometry of both labeled and unlabeled cytochrome b_5 was provided by Dr. Bradford Gibson at the UCSF Mass Spectrometry Facility (A. L. Burlingame, Director) supported by the Biomedical Research Technology Program of the National Center for Research Resources, NIH NCRR BRTP 01614. We thank Dr. Steve Sligar for providing the puc13 plasmic containing the synthetic gene coding for rat cytochrome b_5. We thank Dr. Richard Shand for providing the host strain of *E. coli* (NCM 533) which greatly enhanced the expression yield in minimal media. We thank Drs. Gerd La Mar and S. Donald Emerson for providing the dipolar shift calculation program. We are grateful to the Computer

Graphics Laboratory at UCSF for the use of the facilities in the display and interpretation of the crystallographic data. We are indebted to Dr. Michael Summers for the use of his General Electric OMEGA PSG-600 NMR spectrometer and for much advice and assistance in the acquisition and processing of spectra using current pulse technology.

REFERENCES

Argos, P., & Mathews, F. S. (1975) *J. Biol. Chem. 250*, 747–751.

Bax, A., & Davis, D. G. (1985) *J. Magn. Reson. 65*, 355–360.

Bax, A., Griffey, R. H., & Hawkins, B. L. (1983) *J. Magn. Reson. 55*, 355–360.

Bertini, I., & Luchinat, C. (1986) *NMR of Paramagnetic Molecules in Biological Systems*, pp 19–81 and 253–262, Benjamin/Cummings Publishing, Menlo Park, CA.

Bodenhausen, G., Vold, R. L., & Vold, R. R. (1980) *J. Magn. Reson. 37*, 93–106.

Bois-Poltoratsky, R., & Ehrenberg, A. (1967) *Eur. J. Biochem. 2*, 361–365.

Bovey, F. A. (1988) *Nuclear Magnetic Resonance Spectroscopy*, pp 460–469, Academic Press, New York.

Brown, S. C., Weber, P. L., & Mueller, L. (1988) *J. Magn. Reson. 71*, 166–171.

Bundi, A., & Wüthrich, K. (1979) *Biopolymers 18*, 285–298.

Dyson, H. J., Holmgren, A., & Wright, P. E. (1988) *FEBS Lett. 228*, 254–258.

Emerson, S. D., & La Mar, G. N. (1990) *Biochemistry 29*, 1556–1566.

Feng, Y., Roder, H., & Englander, S. W. (1989) *Biochemistry 28*, 195–203.

Feng, Y., Roder, H., & Englander, S. W. (1990a) *Biophys. J. 57*, 15–22.

Feng, Y., Roder, H., & Englander, S. W. (1990b) *Biochemistry 29*, 3494–3504.

Gao, Y., Boyd, J., Pielak, G. J., & Williams, R. J. P. (1991) *Biochemistry 30*, 1928–1934.

Gippert, G. P., Yip, P. F., Wright, P. E., & Case, D. A. (1990) *Biochem. Pharmacol. 40*, 15–22.

Glushka, J., Lee, M., Coffin, S., & Cowburn, D. (1989) *J. Am. Chem. Soc. 111*, 7716–7722.

Golding, R. M., & Stubbs, L. C. (1979) *J. Magn. Reson. 33*, 627–647.

Griesinger, C., Otting, G., Wüthrich, K., & Ernst, R. R. (1988) *J. Am. Chem. Soc. 110*, 7870–7872.

Guiles, R. D., Altman, J., Lipka, J. J., Kuntz, I. D., & Waskell, L. A. (1990) *Biochemistry 29*, 1276–1279.

Guiles, R. D., Basus, V. J., Kuntz, I. D., & Waskell, L. A. (1992) *Biochemistry 31*, 11365–11375.

Horrocks, W. D., Jr., & Hall, D. D. (1971) *Coord. Chem. Rev. 6*, 147–186.

Horrocks, W. D., Jr., & Greenberg, E. S. (1973) *Biochim. Biophys. Acta 322*, 38–44.

Keijzers, C. P., & de Boer, E. (1975a) *Mol. Phys. 29*, 973–1006.

Keijzers, C. P., & de Boer, E. (1975b) *Mol. Phys. 29*, 1007–1020.

Keller, R. M., & Wüthrich, K. (1972) *Biochim. Biophys. Acta 285*, 326–336.

Kricheldorf, H. R. (1981) *Org. Magn. Reson. 15*, 162–177.

Kurland, R. J., & McGarvey, B. R. (1970) *J. Magn. Reson. 2*, 286–301.

Lenkinkski, R. E. (1984) in *Biological Magnetic Resonance* (Berliner, L. J., & Reuben, J., Eds.) Vol. 6, pp 23–71, Plenum Press, New York.

Llinás, M., Horsley, W. J., & Klein, M. P. (1976) *J. Am. Chem. Soc. 98*, 7554–7558.

Mathews, F. S., Levine, M., & Argos, P. (1972) *J. Mol. Biol. 64*, 449–464.

McIntosh, L. P., Griffey, R. H., Muchmore, D. C., Nielson, C. P., Redfield, A. G., & Dalhquist, F. J. (1987) *Proc. Natl. Acad. Sci. U.S.A. 83*, 9443–9447.

Niedhardt, F. C., Bloch, P. L., & Smith, D. F. (1974) *J. Bacteriol. 119*, 736–747.

Nirmala, N. R., & Wagner, G. (1988) *J. Am. Chem. Soc. 110*, 7557–7558.

Ösapay, K., & Case, D. A. (1991) *J. Am. Chem. Soc. 113*, 9436–9444.

Pearson, G. A. (1977) *J. Magn. Reson. 27*, 265–272.

Piantini, O. W., Sørensen, O. W., & Ernst, R. R. (1982) *J. Am. Chem. Soc. 104*, 6800–6801.

Pochapsky, T. C., Sligar, S. G., McLachlan, S. J., & LaMar, G. N. (1990) *J. Am. Chem. Soc. 112*, 5258–5263.

Redfield, A. G., & Gupta (1971) *Cold Spring Harbor Symp. Quant. Biol. 36*, 405–411.

Redfield, A. G., & Kunz, S. D. (1975) *J. Magn. Reson. 19*, 250–254.

Scullane, M. I., Taylor, R. D., Minelli, M., Yamanouchi, K., Enemark, J. H., & Chasteen, N. D. (1979) *Inorg. Chem. 18*, 3213–3219.

Shaka, A. J., & Freeman, R. (1983) *J. Magn. Reson. 51*, 169–173.

Shaka, A. J., Keller, J., Frenkiel, T. A., & Freeman, R. (1983) *J. Magn. Reson. 52*, 335–338.

Shand, R. F., Meircke, L. J. W., Mitra, A. K., Fong, S. K., Stroud, R. M., & Betlach, M. C. (1991) *Biochemistry 30*, 3082–3091.

States, D. J., Haberkorn, R. A., & Ruben, D. J. (1982) *J. Magn. Reson. 48*, 286–292.

Strittmatter, P., & Velick, S. F. (1956) *J. Biol. Chem. 221*, 253–264.

Veitch, N. C., Whitford, D., & Williams, R. J. P. (1990) *FEBS Lett. 269*, 297–304.

Villafranca, J. J. (1989) *Methods Enzymol. 177*, 403–413.

von Bodman, S. B., Schulder, M. A., Jollie, D. R., & Sligar, S. G. (1986) *Proc. Natl. Acad. Sci. U.S.A. 83*, 9443–9447.

Walker, F. A., Emrick, D., Rivera, J. E., Hanquet, B. J., & Buttlaire, D. H. (1988) *J. Am. Chem. Soc. 110*, 6234–6240.

Wand, A. J., DiStefano, D. L., Feng, Y., Roder, H., & Englander, S. W. (1989) *Biochemistry 28*, 186–194.

Weissbluth, M. (1967) *Struct. Bonding 2*, 84–90.

Williams, G., Clayden, N. J., Moore, G. R., & Williams, R. J. P. (1985) *J. Mol. Biol. 183*, 447–460.

Wüthrich, K. (1986) *NMR of Proteins and Nucleic Acids*, Wiley, New York.

Zuiderweg, E. R. P., Hallenga, K., & Olejniczak, E. T. (1986) *J. Magn. Reson. 70*, 336–343.